

H.J.Axon and M.J.Nasir The Bondoc meteorite M1

A metallographic and microprobe examination of a metallic nodule from the Bondoc Peninsula meteorite

H.J. Axon and M.J. Nasir, Metallurgy Department, University of Manchester, England.

Introduction

Preliminary accounts of the Bondoc Peninsula (B.P.) meteorite by Krinov (1962) and Ninninger (1963) record a badly corroded condition and describe a unique structure of 70% stony class material; 17% stony-iron (mesosiderite) class material and 11% iron class material. The iron class material was present as metallic "Nodules" of several centimetres diameter, embedded in stony-iron material. There appears to be no previous metallographic study of these centimetre size metallic nodules. We now report a metallographic and microprobe study of one such nodule and of some of the small oxide-silicate-phosphate inclusions that are present within the metal together with a note on banded olivine crystals in the silicate matrix.

Powell (1969) (1971) studied the metal and silicate phases of a number of conventional mesosiderites. He reported bulk metal compositions in the range 7.5 to 8.8 wt.% Ni and he used the method of Wood (1967) to evaluate cooling rates of about $0.1^{\circ}\text{C}/\text{Myr}$ for the compositionally zoned taenite. Powell (1969) showed that central Ni contents in the taenite varied between 40 and 50 wt.% Ni and in the kamacite between 6 and 4 wt.% Ni as the diameter of the metal particles decreased from about 40 μm . Larger particles gave lower (taenite) or higher (kamacite) values. On the basis of recrystallisation effects in the silicate structures Powell (1971) designated three classes of increasing metamorphic reheating. Unfortunately Powell's sample of B.P. was too badly corroded to allow him to determine either cooling rate or metamorphic class. Wasson, et al. (1974) made chemical analyses of the metal in a number of mesosiderites and drew attention to a chemical similarity between mesosiderites and the so-called irons-with-silicate-inclusions. They indicated that the metal of B.P. had a composition appropriate to Powell's higher metamorphic classes and they reported an unusual positive correlation between Ir and Ni. However this correlation depends on Ni measurements that scatter somewhat within a single meteorite and it vanishes if the later Ni analyses of Begemann, et al. (1976) are accepted.

Present work: Experimental methods and results

We examined a slice (measuring 2.3×1.5 cm and weighing 16.8 g) from a metallic nodule of B.P. (# (2) 684.166 - American Meteorite Laboratory) using conventional metallographic and microprobe methods. Metal phase analyses were conducted with an A.E.I. microprobe using carbon coated samples and standard alloys. In addition some analyses of silicate, phosphate and opaque mineral phases were undertaken with a Geacscan microprobe. We also made limited petrological observations on a thin section of olivine taken from a silicate rich sample of B.P. obtained from the same source.

Figure 1 shows part of our metallic nodule. A small amount of stony-iron material adheres to the outside of the metal and embedded within it there are numerous non-metallic inclusions that range in size from 0.5 to 1.5 mm. These inclusions may be classified as angular, Fig. 2, or globular, Fig. 3. However, in many instances the inclusions show varieties of structure intermediate between the extremes of Figs. 2 and 3 and in most instances the situation is further complicated by excessive terrestrial alteration of the silicate and corrosion of the metal at the metal-inclusion interface. In the present work inclusions of unambiguous structure and as free as possible from terrestrialization were selected.

The macrostructure of the metallic nodule, Fig. 1, consists of a polycrystalline array of kamacite grains that are equant in shape and about 3-4 mm. diameter. The angular and globular inclusions are found equally at kamacite grain boundaries and within the kamacite grains of Fig. 1. Most of the boundaries between kamacite grains are heavily invaded by terrestrial corrosion product. Detailed microscopic examination suggests that these grain-boundary locations originally contained films of schreibersite, which has cracked in a brittle manner and consequently allowed the deep intergranular penetration of corrosion. Strips of compositionally zoned taenite are still present, in association with schreibersite, at some of the kamacite grain boundaries and, on deep etching with Nital, show structureless white outer bands followed by a reticulated version of Scott's (1973) cloudy taenite; at the centre of some of the wider strips there may be a diffused acicular structure similar to well-tempered

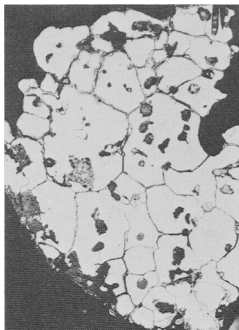


Fig. 1.

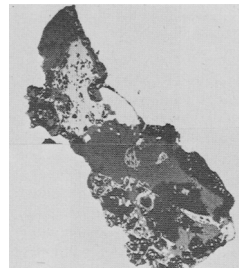


Fig. 2.

Fig. 1. Unetched macrosection of the metallic nodule, showing angular and globular inclusions in polycrystalline kamacite. There is extensive penetration of terrestrial corrosion product along the kamacite grain boundaries. Taenite and schreibersite are present at kamacite boundaries. Field of view 1.6 cm x 2.2 cm. Angular inclusion Fig. 2 is located in the lower-left quadrant and globular inclusion Fig. 3 is located towards the bottom centre of Fig. 1.

Fig. 2. Polymineralic angular inclusion containing large areas of chromite (uneven, light grey) and tridymite (smooth, dark), with small metal particles (white) forming a belt near the major tridymite-chromite boundary. These particles of metal were free from corrosion and their analyses are reported in Fig. 5. A large wart of compositionally zoned taenite abuts the major chromite field and is separated from the kamacite matrix by a thin band of (dark) corrosion product. Unetched. The true length of the inclusion is 1.6 mm.

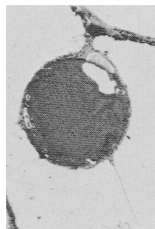


Fig. 3.

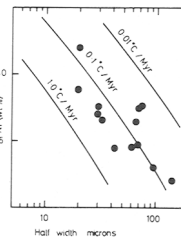


Fig. 4.

Fig. 3. Opalescent globular inclusion showing a radiating feathery structure of whitlockite in devitrified glass. The metal particles are concentrated in a rim around the edge of the globule. Light Nital etch. True diameter 0.7 mm.

Fig. 4. Composition-dimension relationship for zoned taenite in the metallic nodule of Bondoc. Cooling rate curves from Powell (1969).

martensite. Chunky fields of similarly zoned taenite are found at kamacite triple points. Smaller areas of compositionally zoned cloudy taenite are encountered as wart-like incrustations at the surface of both angular and globular inclusions. Occasionally zoned wart material appears within globular type inclusions, Fig. 3. Schreibersite also is occasionally encountered in wart form. Idiomorphic bodies of zoned taenite and of schreibersite are encountered on rare occasions, without silicate associations, within kamacite grains, suggesting either the coalescence of identically oriented neighbouring grains of kamacite or the migration of kamacite grain boundaries after the zoned taenite and schreibersite had developed. Within the metal as a whole the taenite and schreibersite each contribute 2% by volume. Their average Ni contents (from data reported later) appear to be 440 wt.% and 445 wt.% Ni respectively. The average of microprobe counts in the kamacite matrix gives 5.2 wt.% Ni; 0.75 wt.% Co;

0.02 wt.% P and when this is taken with the observed proportions and compositions of taenite and schreibersite it yields a calculated bulk composition of the metal at ~ 7.5 wt.% Ni; ~ 0.7 wt.% Co; ~ 0.3 wt.% P, which is in reasonable agreement with Powell's (1969) bulk analysis of 7.4 wt.% Ni and the Begemann et al. (1976) value of 7.5-7.6 wt.% Ni.

Attention has been drawn to the corrosion problem in B.P. At the interface with zoned taenite corrosion is concentrated in the kamacite and usually a 5-10 μm layer of corrosion product prevents the investigation of Agrell type Ni-concentration profiles in the kamacite. However, for the zoned taenite reasonably satisfactory central Ni contents and half-widths may usually be determined and Fig. 4, plotted according to the method of Wood (1967) as employed by Powell (1969) shows our results. The lower envelope of the experimental points indicates an effective cooling rate slightly more rapid than that of $0.1^\circ\text{C}/\text{Myr}$ which Powell (1969) determined by the same procedure on a number of other mesosiderites. The average Ni content of zoned taenite in our sample is $\sim 40\%$ Ni. Three uncracked idiomorphic particles of phosphide were examined and analysed at 49; 46.5 and 40.5 wt.% Ni respectively for widths of 50; 40 and 150 μm . Phosphide of such high Ni content would be formed late in the cooling process and indicates a low equilibration temperature. No conventional rhodites were observed. Neumann bands appear in the kamacite of our sample when etched in Nital; they are usually narrow and straight sided and occasionally they are broken up into segments like a dashed or broken line. These features are consistent with a mild heat treatment after the Neumann bands had formed. From annealing experiments with Cañon Diablo material a heat-treatment temperature below about 500°C seems to be indicated, since the recrystallisation of Neumann intersections reported by Axon (1967) at 550°C was not observed.

The mineralogy of the inclusions within the metal differs for angular and globular varieties. Angular inclusions are coarsely crystalline and the most common type contain massive chromite and tridymite crystals with pyroxene, anorthite and whitlockite usually present as well. Most angular inclusions also contain small particles of metal, 10-40 μm dia, that are interstitially located with respect to the mineral phases and

distributed throughout the depth of the inclusion. Small quantities of sulphide and phosphide are similarly located. Fig. 5 shows a number of Ni and Co analyses conducted on the metal particles within two angular inclusions of the type shown in Fig. 2. In this plot the analysis points are taken from uncorroded metal of maximum diameter 40 μm and all analyses show <0.1 wt.% P. In general the single phase kamacite or taenite particles within the angular inclusions are chemically homogeneous. In one instance a metal particle with a two phase structure of kamacite and clear taenite was encountered and these co-existing metal-phase compositions are joined by a tie-line in Fig. 5.

By contrast the opalescent globular inclusions are free of chromium, are microcrystalline and show radiating feathery crystals of whitlockite in a background of devitrified glass. In the hand specimens these globules have a milky-white opalescent appearance which is also obtained by microscopic examination in polarised reflected light. Metallic, phosphide and sulphide particles are usually distributed in a concentric zone within the rim of the globule. If zoned taenite is excluded the metallic particles usually have diameters <10 μm and appear compositionally homogeneous. Analyses of such metal at the rims of four opalescent globular inclusions are collected in Fig. 6. These are point analyses on particles of metal that are small in size and apparently chemically homogeneous. However, in one instance two point analyses could be made on Ni-rich and Ni-poor phases in the same particle, and these are plotted as a tie-line on Fig. 5, where an attempt is also made to distinguish between particles that show compositions appropriate to conventional kamacite or taenite (open symbols) and other particles whose compositions appear more appropriate to a duplex plessitic structure (filled symbols). Unfortunately the latter particles are too small to show structural detail but if they are two phase on a sub-microscopic scale they would be analogous to the zoneless plessites that Sears and Axon (1975) have noted in the chondrules of Barwell and other stony meteorites. The metal particles analysed for Fig. 6 have P contents in the range 0.2-0.4 wt.% P. All the globules in Fig. 6 have rather similar structures and compositions in both metallic and non-metallic portions. The average or bulk composition of the central, metal-free, portions of these globules is very similar and averages 5 MgO; 15 Al_2O_3 ; 54 SiO_2 ; 13 CaO; 8 P_2O_5 ; 3 FeO; 1 TiO_2 with no detectable Cr_2O_3 .

Attention has so far been directed to polymineralline angular inclusions with massive chromite, Fig. 2, and to opalescent globules without Cr_2O_3 , Fig. 3. These represent the extreme types, for which multiple examples may be identified within our module. In addition we have encountered single examples of different structures such as (I) an opalescent globule with one central body of metal consisting of two phases for which the co-existing compositions were kamacite 4.3 Ni; 0.5 Co and taenite 50 Ni; 0.14 Co; (II) a non-opalescent globule with many peripheral inclusions of taenite containing ~ 41 Ni; 0.2 Co; (iii) an angular single crystal of anorthite, embedded in schreibersite, free of chromite but containing small particles of metal of about 8 wt.% Ni, >0.2 wt.% P and with Co variable between 0 and 0.18 wt.% (IV) a complex range of polymineralline partly globular-partly angular inclusions, most of which were badly penetrated by corrosion product and for which systematic and reliable analyses could not be made.

In addition to the detailed study of the metallic nodule and its inclusions a petrographic thin section was prepared from a large olivine crystal that was present in a metal-free area of another sample. The olivine showed the well developed banding that Powell noted in a number of mesosiderites and which are consistent with slow deformation of the olivine at a temperature of $1000-1300^\circ\text{C}$. Similar banded olivines have been discussed by Hamilton (1957) in some Scottish carboniferous olivine-basalts.

Discussion

The distribution of kamacite, zoned taenite, schreibersite and non-metallic inclusions in Fig. 1 is consistent with the following thermal history:- at temperatures above 750°C the metallic nodules consisted of angular, globular and intermediate types of inclusion randomly distributed within chemically homogeneous volumes of parent taenite containing ~ 7.5 wt.% Ni; ~ 0.3 wt.% P. Slow cooling from this temperature into the $\alpha+\gamma$ region of the equilibrium diagram allowed kamacite to nucleate at favourable locations on some of the inclusions. On further cooling this kamacite developed by the usual process of diffusion-controlled growth, the final limits of kamacite growth are marked out in the macrostructure by the fields of zoned taenite and by the grain boundary schreibersite. There is no detectable chemical difference between the major proportion of zoned

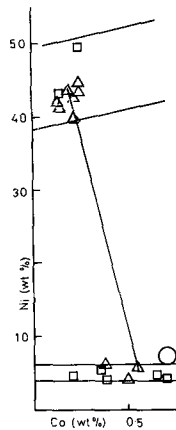


Fig. 5.

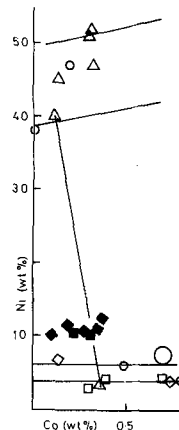


Fig. 6.

Fig. 5. Plot of the Ni and Co contents of metallic particles within two angular polymineralline inclusions. Triangles represent data from Fig. 2. Tie-line joins kamacite and taenite compositions in a two-phase particle. Composition bands are drawn for the variation of Ni content with particle size (Fig. 4) that is to be expected for kamacite and taenite in the measured size-range. The large circular symbol represents the calculated bulk composition of the metallic nodule, Fig. 1.

Fig. 6. Plot of the Ni and Co contents of metallic particles in the rim zones of four opalescent globular inclusions. Large circle, tie-line and composition bands have the same significance as in Fig. 5. Full symbols represent "plessitic" compositions.

taenite that occurs at kamacite grain boundaries;

the small quantity within kamacite grains or the somewhat larger quantity that occurs as wart-like residues on some of the non-metallic inclusions. These warts of zoned residual taenite clearly indicate that kamacite did not nucleate and grow concentrically round each of the inclusions and in this respect the situation is different from the smacking kamacite that surrounds sulphide and other bodies in octahedrite iron meteorites.

Zoned taenite forms in the first phase by the process of continuous retreat during slow continuous cooling and, provided that the concentration profiles are not distorted by later reheating, may be used to evaluate cooling rates. The rate evaluated for our material is slightly more rapid than the value of $0.1^{\circ}\text{C}/\text{Myr}$, which Powell (1969) obtained for other mesosiderites but in B.P. there is some metallographic evidence of reheating, in particular the disjointed Neumanns and reticulated cloudy taenite. The effective temperature of equilibration during the initial slow cool may be given by the α - γ interface compositions. Unfortunately α interfaces are destroyed by corrosion but peak Ni values in excess of 50 wt.% are determined at the edge of zoned taenite and according to Goldstein and Ogilvie's (1965) binary Fe-Ni equilibrium diagram such a nickel content corresponds to equilibration at temperatures about 350°C . An alternative measure of equilibration on slow cooling may be obtained from the P content of the kamacite matrix, which, at 0.02 wt.% P corresponds to 350°C in the Fe-Ni-P equilibrium diagram of Doan and Goldstein (1970). It thus appears that the massive metal of B.P. had an early history of slow cooling to an effective equilibration temperature of $\sim 350^{\circ}\text{C}$.

By contrast the small two-phase $\alpha\gamma$ structures that have been encountered within the metal of the angular or globular inclusions show Ni-Co tie-line relationships that are appropriate to temperatures of $\sim 450^{\circ}\text{C}$ on the binary Fe-Ni equilibrium diagram. The taenite in these two phase particles is small and apparently homogeneous and it is probably isothermal taenite produced by reheating in the manner described originally by Brentnall and Axon (1962). If this is so the reheating temperature is consistent with the value of $\sim 500^{\circ}\text{C}$ derived from metallographic indicators and would operate for periods of weeks, not years.

Insofar as composition is concerned the small particles of metal within the angular polymersilicic-chromite-containing inclusions of Fig. 5 appear to be of different Ni, Co and P content from the metal within the single angular inclusion of chromium free anorthite [~ 8 Ni; 0-0.16 Co; >0.2 P] and may have had a different origin. Thus it appears that angular inclusions may be present from at least two sources.

The small metal particles that occur in the rim zone of the opaque-globular inclusions show three ranges of composition on the Ni-Co plot. In addition to the straight kamacite and taenite ranges there is also metal of intermediate or pleissitic composition and this is plotted as filled symbols. The range of metal compositions in the globules would be consistent with metal from angular types of inclusion that had been remelted (perhaps by shock) and redistributed as metallic particles within the molten silicate-phosphate globules.

In both Figs. 5 and 6 the calculated bulk composition of the metallic nodule is indicated by a large circular symbol, from which it appears that the small particles of metal within the angular (or globular) inclusions are of different Co content and therefore, presumably, of different origin from the metal that forms the main mass of the nodule. It may also be noted in Figs. 5 and 6 that the single phase kamacite particles occupy a range of Ni contents between 4 and 6 wt.% and this is consistent with the trend that Powell observed between Ni content and size for metal particles of this size range in mesosiderite metal-silicate assemblages. However, Powell did not report Co contents and the present results show that an arrangement of kamacite compositions along the single phase α boundary of the ternary Fe-Ni-Co diagram is superimposed upon the previously established relationship between particle size and Ni content.

Similar remarks apply to the single phase taenite compositions that are recorded in Figs. 5 and 6, although in this case the Ni content has been shown to vary more steeply with particle size. The evidence of Figs. 5 and 6 is consistent with a γ phase boundary in the Fe-Ni-Co system that extended to slightly higher Ni contents as the Co content was increased. The parallel limits of the trend-band for taenite in Figs. 5 and 6 are constructed primarily by reference to the plotted points but they are also consistent with a large number of additional analyses for which the P content or extent of corrosion is greater or for which the silicate association

is more ambiguous.

The exact mechanism by which a range of globular and angular inclusions was emplaced within the nodule of metal is not easy to specify. Shock emplacement seems to be an attractive possibility but in order to accommodate in the inclusions a range of reheating effects varying from the completely melted extreme of the globular type, Fig. 3, to the un-melted high-chromite type, Fig. 2, it appears necessary to assume that the shock was not excessively severe. This condition would be satisfied if the temperature of the metal was sufficiently high immediately before the shock event. The exact pre-shock temperature is not certain. It was probably in the γ range and sufficiently high to allow the metal of the nodule to grow into a single crystal of γ after the inclusions were emplaced, but, in view of the absence of compositionally zoned solidification structures in the nodule it is unlikely that the metal was itself melted during the shock-emplacement event.

Thus the structural evidence of the metallic nodules is consistent with the suggestion of Wasson et al. (1974) that a relatively mild shock event contributed to the formation of the mesosiderites and it is now possible to indicate, for B.P., a pre-shock temperature in the γ range for the metal of the nodules. The total history of B.P. is complicated by the need to accommodate the observation of massive banding in some of its olivine crystals, which seems to indicate a slow, creep-like deformation of the massive silicates at temperatures in excess of 1000°C . This creep deformation could have taken place subsequent to the emplacement of silicates within the nodules and the incorporation of the metallic nodules into the stony matrix of the meteorite. Finally, the presence of partly annealed Neumann bands in the metallic nodules indicates an impact late in the history of the meteorite, followed by a final short reheating to $\sim 450^{\circ}\text{C}$ before terrestrial corrosion became important.

The unique structure of Bondoc Peninsula that was noted in the preliminary reports of Krinov (1962) and Ringer (1963) is to be set against the observations of smaller metal-silicate nodules in the more conventional mesosiderites Mincy, Morristown, Crab Orchard and Estherville [figured by Powell (1971)] and banded olivines in Morristown, Veramin, Vaca Muerta and Crab Orchard, Powell (1971). The analyses of Wasson et al. (1974) place Bondoc Peninsula among the mesosiderites and the present observations of metal cooling rates and compositions are consistent with other mesosiderites if allowance is made for the uncertainties introduced by the late-stage reheating and corrosion of Bondoc Peninsula material.

Acknowledgements. Our thanks are due to colleagues in the Geology Department for Geocron and petrological assistance.

REFERENCES

- Axon (H.J.), 1967. *Metals and Materials*, 1, 82.
 Begenmann (F.), Weber (R.W.), Vilcek (E.) and Hintenberger (H.), 1976. *Geochim.Cosmochim.Acta*, 40, 353.
 Brentnall (W.D.) and Axon (H.J.), 1962. *J.Iron Steel Inst.*, 200, 947.
 Doan (A.S.) and Goldstein (J.I.), 1970. *Metal Trans.*, 1, 1759.
 Goldstein (J.I.) and Ogilvie (R.E.), 1965. *Trans.Metall.Soc.A.I.M.E.*, 233, 2083.
 Hamilton (J.), 1957. *Geol.Mag.*, 34, 135.
 Krinov (E.L.), 1962. *The Meteoritical Bulletin No. 25*, p.3.
 Ringer (H.E.), 1963. *Science*, 139, 345.
 Powell (B.J.), 1969. *Geochim.Cosmochim.Acta*, 33, 789.
 " 1971. *Ibid.*, 35, 5.
 Scott (E.R.D.), 1973. *Ibid.*, 37, 2283.
 Sears (D.W.) and Axon (H.J.), 1975. *Meteoritics*, 10, 486.
 Wasson (J.T.), Schandy (R.), Blid (R.W.) and Chou (C-L.), 1974. *Geochim.Cosmochim.Acta*, 38, 135.
 Wood (J.A.), 1967. *Taurus*, 6, 1.